LRD - ORNL - RC

APR 28 1980

DATE ISSUED

OAK RIDGE NATIONAL LABORATORY
OPERATED BY
UNION CARBIDE CORPORATION
NUCLEAR DIVISION
POST OFFICE BOX X
OAK RIDGE, TENNESSEE 37830

Special Distribution

ORNL
CENTRAL FILES NUMBER
ORNL/CF-80/77

800423

DATE: April 18, 1980

SUBJECT: Technical Highlights of Space and Terrestrial Systems Programs at Oak Ridge National Laboratory for February 1980

TO: Distribution

FROM: A. C. Schaffhauser

This monthly report is intended to inform the Division of Advanced Nuclear Systems and Projects, DOE, and their contractors of significant technical highlights of technology and systems support programs in progress at Oak Ridge National Laboratory. A detailed technical presentation of information will be published in topical reports and open literature publications.

[redacted]

CONTENTS

SOLAR-POLAR MISSION MATERIALS SUPPORT 1

CBCF-3 Insulation Fabrication 1
Contact Conductance Measurements at Purdue 1
Contact Conductance Measurements at ORNL 3
Important Meetings 4

FLIGHT SYSTEMS HARDWARE 5

Iridium Blank Fabrication 5
Recrystallization in Ir-0.3% W Alloy Sheet 7

MATERIALS TECHNOLOGY SUPPORT 10

Effect of Phosphorus Contamination on Impact Properties of DOP-26 and DOP-4 Alloys 10
AES Analysis of P-Doped DOP-26 13
Development of Pt-Base Alloys 13
Impact Behavior of Mo and Mo-Re Alloys 16
Important Meetings 17

ISOTOPE FUEL DEVELOPMENT 18

$^{90}SrF_2$ Compatibility 18

TERRESTRIAL RADIOISOTOPE APPLICATIONS DEVELOPMENT 19

Cesium-137 Low Solubility Compounds 19
Examination of WESF Cesium Capsules 20
Krypton-85 Light Source Development 20

BENEFICIAL APPLICATIONS OF RADIATION TECHNOLOGY 22

SOLAR-POLAR MISSION MATERIALS SUPPORT

(Activity AE 15 15 20 0, WPAS 02313)

R. L. Heestand

The purpose of this task is to provide direct materials support on work specific to the General Purpose Heat Source (GPHS) design. The scope of this work includes (1) determining the impact properties and optimum weld parameters for the DOP26 iridium alloy fuel cladding material, (2) thermal conductivity and emissivity data on cladding and thermal insulation materials, and (3) fabrication and characterization of test samples of carbon-bonded carbon-fiber (CBCF) insulation developed by ORNL and Y-12 which may be used for GPHS. Data on the impact properties and welding of iridium are integrated with complementary work reported in the materials technology section of this report.

CBCF-3 Insulation Fabrication (G. C. Wei and G. W. Brassell)

Multiple molding using nine mandrels simultaneously for preproduction and production of CBCF-3 cups was initiated. Initial deposits appeared to be successful and are being carbonized. In addition, flat plate samples were deposited for material for end discs. Samples from these runs will be evaluated for properties including preliminary machining, x-ray radiography, DXT, inspection, density and compressive strength measurements. Written procedures of all steps of fabrication and tests are being prepared.

Contact Conductance Measurements at Purdue (G. C. Wei)

The contact conductance measurements using laser flash diffusivity method were initiated at TPRL in October 1979. Conceptual design and construction of apparatus and equipment were largely completed by December 1979. Outgassed samples including FWPF 3D CC, PG, CBCF-3, Ir, and grafoil were sent to TPRL on December 20, 1979. On January 31, 1980, we received preliminary results shown in Table 1. Since then, some members of the GPHS design group expressed their concern about the magnitude of the experimentally determined contact conductance. In the meantime, specimens were also delivered to Carl Alexander of BCL who conducted both laser flash and longitudinal heat flow measurements. The preliminary results (Table 2) of BCL's measurements are generally lower than Purdue's. ORNL is also working on it using a longitudinal heat flow method (see next section).

In order to resolve the discrepancy in the two sets of data, we visited Dr. Taylor of TPRL on February 14, 1980. The following possible sources of error were identified and their contributions to the uncertainty in the contact conductance data were under investigation.

Table 1. Preliminary Contact Conductance Data from Ray Taylor of Purdue Using Laser Flash Method and Lee's Model

Material System	Temperature (°C)	Contact Pressure (psi)	Environment	Contact Conductance ($W/cm^2 \cdot K$)
FWPF (Z⊥) vs FWPF (Z ‖)	RT	5	10^{-3} torr	1.3
	RT	75	10^{-3} torr	5.3
	RT	175	10^{-3} torr	22.
	RT	5	0.1 atm air	1.58
	RT	75	0.1 atm air	6.3
	RT	175	0.1 atm air	22.
	300°C	5	0.1 atm air	1.52
	300°C	>75	0.1 atm air	32.
	300°C	>175	0.1 atm air	690.
PG vs FWPF (Z ‖)	RT	5	10^{-3} torr	0.8
	RT	75	10^{-3} torr	32.
	RT	150	10^{-3} torr	large
	RT	5	0.1 atm air	0.85
	RT	75	0.1 atm air	34.
	RT	150	0.1 atm air	large
PG vs FWPF (Z⊥)	RT	5	10^{-3} torr	0.30
	RT	75	10^{-3} torr	1.52
	RT	175	10^{-3} torr	3.0
	RT	5	0.1 atm air	0.45
	RT	75	0.1 atm air	1.5
	RT	175	0.1 atm air	2.9
FWPF (Z⊥) vs Grafoil (0.010-in. thick)	RT	5	10^{-3} torr	0.84
	RT	75	10^{-3} torr	1.56
	RT	175	10^{-3} torr	1.85
	RT	5	0.1 atm air	0.59
	RT	75	0.1 atm air	1.3
	RT	175	0.1 atm air	1.92
Ir vs FWPF (Z⊥)	RT	5	10^{-3} torr	0.38
	RT	75	10^{-3} torr	7.7
	RT	175	10^{-3} torr	11.
	RT	5	0.1 atm air	0.6
	RT	75	0.1 atm air	7.9
	RT	175	0.1 atm air	12.8
PG vs PG	RT	5	10^{-3} torr	0.28
	RT	75	10^{-3} torr	large
	RT	175	10^{-3} torr	large
	RT	5	0.1 atm air	0.94
	RT	75	0.1 atm air	large
	RT	175	0.1 atm air	large
Ir vs Grafoil (0.40-in. thick)	RT	5	10^{-3} torr	0.92
	RT	75	10^{-3} torr	large
	RT	175	10^{-3} torr	large
	RT	5	0.1 atm air	1.19
	RT	75	0.1 atm air	large
	RT	175	0.1 atm air	large
	300°C	5	0.1 atm air	1.85
	300°C	75	0.1 atm air	large
	300°C	175	0.1 atm air	large
CBCF-3 vs FWPF (Z⊥)	RT	5	10^{-3} torr	0.016
	RT	75	10^{-3} torr	large
	RT	175	10^{-3} torr	large
	RT	5	0.1 atm air	0.27
	RT	75	0.1 atm air	large
	RT	175	0.1 atm air	large

Table 2. Preliminary Contact Conductance Data from Carl Alexander of BCL Using Longitudinal Heat Flow Method

Material	Temperature (°C)	Contact Pressure	Environment	Contact Conductance ($W/cm^2 \cdot K$)
FWPF(Z⊥) vs FWPF(A⊥)	1000	75 psi	vacuum	0.6 ± 0.2

1. Specific heat and thermal conductivity used in calculation. ORNL logitudinal heat flow (RT) values of thermal conductivity of FWPF are 10–20% higher than Purdue's.

2. Half-time (rise time to reach equilibrium at back face) was used in analysis, but one-third time or two-third time should also be checked.

3. Mathematical method. For high pressures, a different method changes the results by ±2×.

4. Non-uniform contact pressure.

5. Transient and steady state conductances may be inherently different.

TPRL measured some literature contacts including Cu-Cu and stainless to stainless steel. The results for Cu-Cu at room temperature and 5 psi contact pressure were in accord with literature data. However, a stronger pressure dependence than those reported in the literature was observed, and the stainless steel data were inconsistent with literature values.

Contact Conductance Measurements at ORNL (R. K. Williams)

Room temperature contact conductance data on FWPF (⊥) vs FWPF (||) interfaces were obtained in two sets of steady-state longitudinal heat flow experiments. The fibers were oriented at a 45° angle in these experiments and all of the data were obtained in vacuum. The surfaces were prepared at ORNL by grinding and the data cover a stress range of 29–160 psi.

The results are shown in Table 3 and indicate that the contact conductance at this interface is unexpectedly high, and tends to increase after cycling to higher stresses. Both methods yield high conductances and these data tend to confirm earlier studies by Purdue using a transient experimental method and samples prepared by LASL.

Table 3. Vacuum Interfacial Conductance of FWPF (⊥) vs FWPF (||)

Test No.	Stress (psi)	Q_{HTR}[a] (w)	$Q_{\perp}$[b] (w)	$Q_{\parallel}$[b] (w)	ΔT_{int} (°C)	$h \frac{watts}{cm^2\ deg}$	Average Temp (°C)
1	55	1.30	1.13	1.11	2.40	1.48	18.15
1	55	2.37	1.98	1.93	4.40	1.41	31.65
2	160	—	1.18	1.18	0.25	15.0	18.04
2	160	—	2.08	2.08	0.45	14.7	31.44
3	55	—	1.17	1.17	0.46	8.0	17.83
3	55	—	2.04	2.02	0.80	8.0	31.87
4	55	—	1.15	1.16	0.50	7.3	17.94
5	29	—	1.13	1.14	1.48	2.42	17.85
1A	100	Indirect measurement using thermal comparator				12.4	60.
	160	Indirect measurement using thermal comparator				9.2	60.

[a]Measured dc voltage drop and current.

[b]Calculated from conductivity and ΔT. Heat flux values were in the range 3.5 to 6.5 watts/cm^2.

Important Meetings

1. R. L. Heestand, G. C. Wei, and G. W. Brassell visited D. Galvin and D. Friedline of MRC to discuss CBCF-3 specification for 1983 Solar-Polar Mission's GPHS, on February 5, 1980.

2. G. C. Wei and R. K. Williams visited Dr. R. E. Taylor of Purdue University on February 14, 1980, to discuss contact conductance experiments relevant to GPHS.

FLIGHT SYSTEMS HARDWARE

(Activity AE 15 20 00 0, WPAS 01322)

D. E. Harasyn

The objective of this task is to supply Mound Facility with flight quality hardware components for use in the assembly of isotope heat sources. The major activity is on fabrication of iridium alloy forming blanks for isotope fuel capsules along with iridium foil for vents, decontamination covers, and weld shields. We have completed fabrication of iridium for the Galileo mission MHW heat source and have initiated fabrication of 1255 iridium blanks and associated foil for Solar-Polar Mission General Purpose Heat Source for delivery in FY 1980 and FY 1981. A new task on fabrication of carbon-bonded carbon-fiber (CBCF) thermal insulation for Light Weight Radioisotope Heating Units (LWRHU) has also been initiated.

Iridium Blank Fabrication (D. E. Harasyn)

Of the 266 blanks that were to have been shipped to MRC by the end of February, 173 have been shipped. Of that 173, 81 (MRC groups 3 and 4) were returned by MRC for recleaning at ORNL to remove microscopic surface inclusions. Seventeen of the 81 were recleaned and shipped to MRC in February, the remainder should be shipped in March. An accelerated fabrication schedule is being implemented to catch up to the MRC requested schedule by July.

X-ray dispersive chemical analyses with SEM at MRC and ORNL indicated that Al and Si were the predominant elements in most of the surface inclusions. This meant that the inclusions most likely originated as small particles which continually break away from the firebrick muffle of the furnace used in the finish rolling process. Although the Ir sheet was stood on edge underneath a Pt-3008 canopy and on top of a Pt 3008 setter plate inside the furnace, the firebrick particles could still transport to the Ir surface presumably by means of air currents when the furnace door was open.

GPHS forming blanks fabricated prior to those from ingot number L239 have been cleaned by our standard cleaning process. This included wire brushing the Ir sheet to help remove imbedded material and to remove an oxide film which would impede electroetching. The sheet was then acid cleaned in HCl + HF. Blanks were cut from the sheet and then washed, electroetched, and finally acid cleaned. Each blank was inspected at 10X to locate and remove inclusions with the tip of a scribe. By this method, most inclusions exceeding 0.06-mm (0.002 in.) diam were removed.

Blanks made from ingot numbers L239 through L263 will be cleaned by immersion in a molten carbonate bath in order to remove aluminosilicate (firebrick inclusions).

The molten carbonate cleaning process consists of the following:

1. Work with batches of about 20 disks.

2. Wash disks with abrasive soap, rinse in tap water assisted with nylon brush.

3. Clean ultrasonically in ethanol for at least 10 min.

4. Individually immerse disks and one surveillance sample in molten carbonate bath for 3 to 3 1/2 min. at 900 ± 20°C. Use new mixture of 50 w/o Na_2CO_3- 50 w/o $K_2CO_3 \cdot 3/2\ H_2O$ for each batch. Use Pt crucible and Pt tipped tongs.

5. When cool, wash with abrasive soap and rinse in warm tap water assisted by nylon brush.

6. Immerse in boiling deionized water for at least 15 min.

7. Immerse in 3 vol HCl - 1 vol HNO_3 for at least 15 min.

8. Return to boiling deionized water bath for at least 5 min.

9. KCN electroetch and acid clean according to Met-MatP-SOP-76, Rev. 6, sequences 15 and 30 (Standard Cleaning Procedure).

Analytical chemists frequently use molten Na_2CO_3 and K_2CO_3 to fuse aluminosilicates in order to dissolve them in water or acids for wet chemical analysis. To test the process with Ir, we sampled an Ir disk containing five inclusions which had not been removed by the standard cleaning procedure. The sample was treated with the molten carbonate process described, removing all visual traces of the inclusions. An energy dispersive x-ray analysis with the SEM showed that the pits where the inclusions had been were as clean as the base metal. Only one pit contained a trace of Fe. At this time 40 blanks have been cleaned by this process and then examined at 10× to 30× with an optical microscope. No inclusions have been observed to remain.

We have completed installation of new WC rolls in a 4-hi rolling mill in our Metals Processing Laboratory. This will allow us to exercise closer control over the finish rolling process which has previously been done at the Y-12 plant on borrowed equipment. We have also set up a new Inconel muffle glo-bar furnace which will be used exclusively for finish rolling Ir sheet. The elimination of firebrick from this furnace is expected to greatly reduce the surface inclusion and pitting problems associated with finish rolling. Blanks made from ingots L264-269 will be the first to be rolled with this new equipment.

Recrystallization in Ir-0.3% W Alloy Sheet (D. E. Harasyn)

Samples from DOP26 Ir-0.3% W production sheets L242R and L247 were annealed at various temperatures to determine their recrystallization curves. The results are shown in Figs. 1 and 2. Samples (5 × 15 mm) were cut from finish rolled Solar Polar production sheet with an abrasive saw. A set of samples (one from L242R and one from L247) was then annealed for 15 min in air at each temperature except for the set annealed at 1400°C, which was annealed in vacuum. The percent recrystallization (Fig. 1), was determined by visually estimating the amount of recrystallization observed in the microstructure of each sample. The microhardness values (Fig. 2), are the average of five readings taken on each sample.

There were no obvious differences between L242R and L247 in their fabrication histories or chemical analyses to explain the almost 50°C difference in recrystallization temperature. However, L242R stuck severely to the Cu mold the first time it was cast. After thorough cleaning, it was remelted and recast. There was no significant increase in Cu content over what is normally detected (5-20 ppm) by SSMS in the final product. The curves for L247 are normal for DOP26 Ir-0.3% W whereas those for L242R are a little higher in temperature than expected. The difference in recrystallization temperature is not expected to be consequential to forming and heat treating operations at MRC.

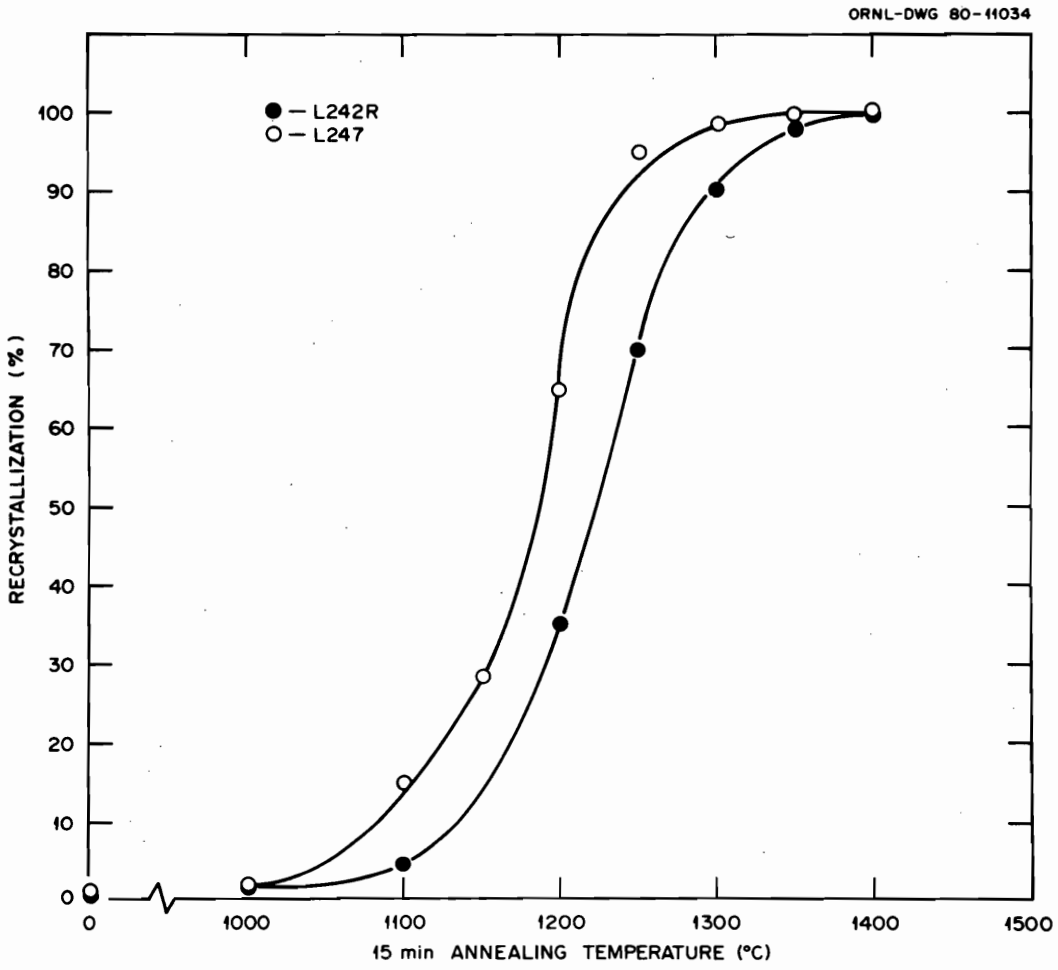

Fig. 1. Percent recrystallization vs annealing temperature for DOP-26 Ir-0.3% W 0.66-mm-thick sheet samples.

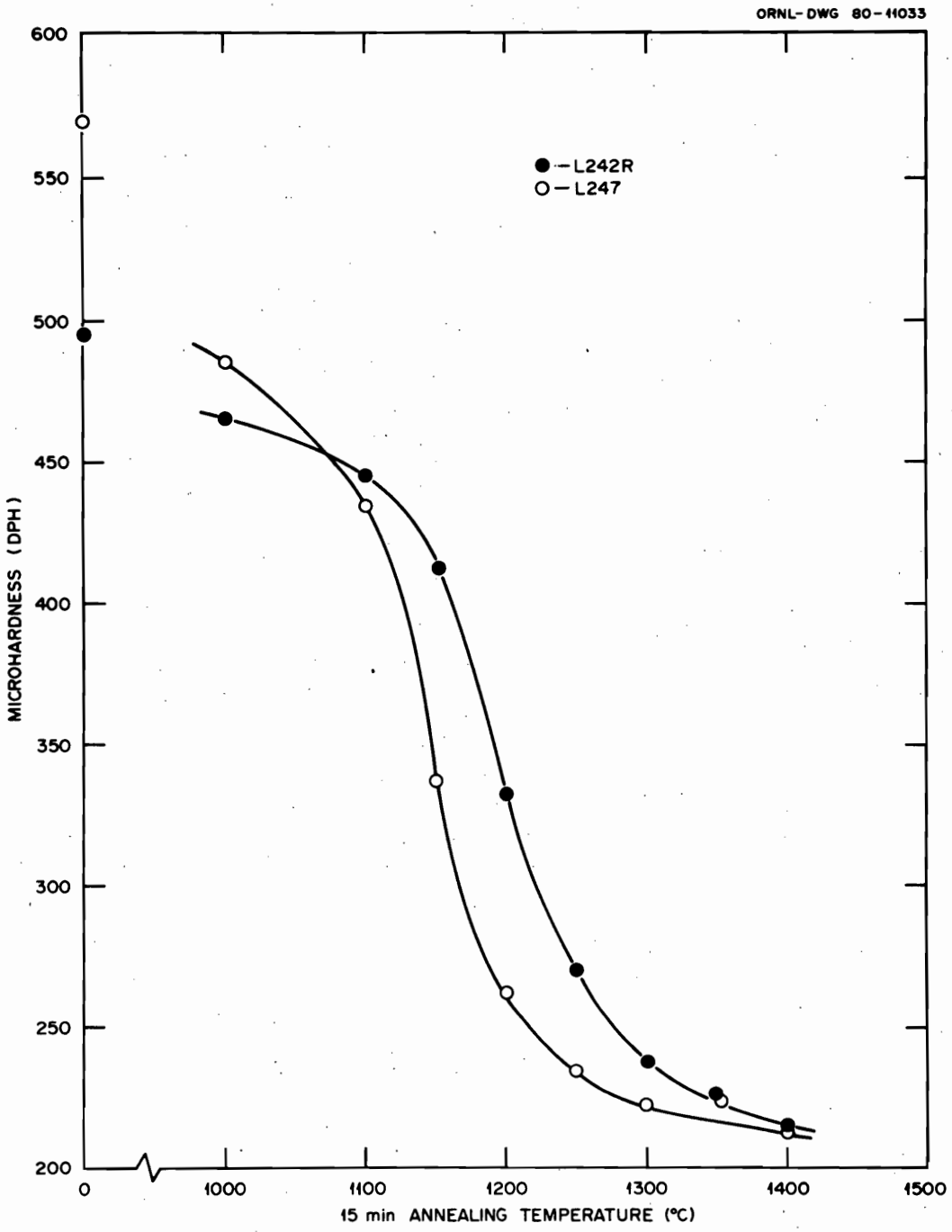

Fig. 2. Microhardness vs annealing temperature for DOP-26 Ir-0.3% W 0.66-mm-thick sheet samples.

MATERIALS TECHNOLOGY SUPPORT

(Activity AE 15 35 00 0, WPAS 01495)

C. T. Liu

The primary objective of this task is to characterize and improve the metallurgical and mechanical properties of noble base alloys, mainly DOP-26 (Ir-0.3% W doped with 60 ppm Th and 50 ppm Al), to meet the requirements of cladding material in radioisotope heat resources for the Galileo and Solar-Polar space missions. The current efforts are concentrated on four areas: (1) to characterize the impact properties of Ir alloys in the temperature range 800–1400°C, (2) to improve the low-temperature impact properties of welds in the DOP-26 alloy, (3) to identify the mechanism and sources that degrade the mechanical and metallurgical properties of doped Ir alloys under heat-source environments, and (4) to develop ductile high-temperature alloys acceptable for future flight missions.

Effect of Phosphorus Contamination on Impact Properties of DOP-26 and DOP-4 Alloys (C. T. Liu and C. L. White)

Table 4 and Fig. 3 summarize the effect of phosphorus contamination on grain size and impact ductility of DOP-26 and DOP-4 alloys. Here, all the specimens were subjected to uniaxial tensile impact tests at 1350°C and 85 m/s (280 fps). The grain size, in terms of number of grains per clad thickness, was measured from the shoulder sections of the impacted specimens. The segregation of phosphorus at the grain boundaries was determined by Auger Electron Spectroscopy (AES) with the P to Ir peak-height-ratio presented in Table 4. The details of AES analysis of the P-doped specimens are reported by C. L. White and R. A. Padgett in the next section.

Figure 3 is a plot of impact elongation and reduction of area as a function of Auger intensity ratio, P(120 eV)/Ir(229 eV). Although only limited data are available at the present time, the plot in Fig. 3 indicates that the impact ductility depends strongly on the level of phosphorus segregated at the grain boundaries. The impact ductility of DOP-26 appears not too sensitive to the level of phosphorus segragation at grain boundaries at a P/Ir ratio <0.3. Above the level, the alloy shows a sharp drop in reduction of area and is completely embrittled with the P/Ir ratio >0.5. As shown in Table 4, the specimens with the P/Ir ratio <0.3 show ductile rupture with close to 100% reduction of area while the specimens with the ratio >0.4 exhibit the brittle grain-boundary fracture. This observation indicates that the loss in ductility of the phosphorus-doped specimens is mainly due to the presence of a significant amount of phosphorus at the grain boundaries, which severely embrittles the boundaries even though thorium is still presented at the boundaries. These results are consistent with results obtained at LASL.

Table 4. Effect of Phosphorus Contamination on Impact Properties of DOP-26 and DOP-4 Alloys Tested at 1350°C and 85 m/s (280 fps)

Alloy	P-Contamination Condition	Heat Treatment	P(120 eV)[a] / Ir(229 eV)	Grain[b] Size	Impact Ductility		
					Elongation	RA[c] (%)	Fracture Model[d]
DOP-26	Uncontaminated	19 h/1500°C/vac	0	14	34-40	94-97	DR
DOP-26	P-doped	18 h/1500°C/vac + 1 h/1500°C/P	0.57	14.1	3.0-5.7	5-7	GBS
DOP-4	P-contaminated[e]	1 h/1500°C/vac	0.43	16.2	20.2	41	GBS
DOP-26	P-doped + Vacuum-Annealed	18 h/1500°C/vac + 1 h/1500°C/P + 2 h/1500°C/vac	0.21	11.8	31.6	94	DR

[a]Average Auger intensity ratio at grain boundaries.

[b]Number of grains per clad thickness.

[c]Reduction of area.

[d]DR = ductile rupture, GBS = grain-boundary separation.

[e]The alloy was contaminated with P during arc melting and casting.

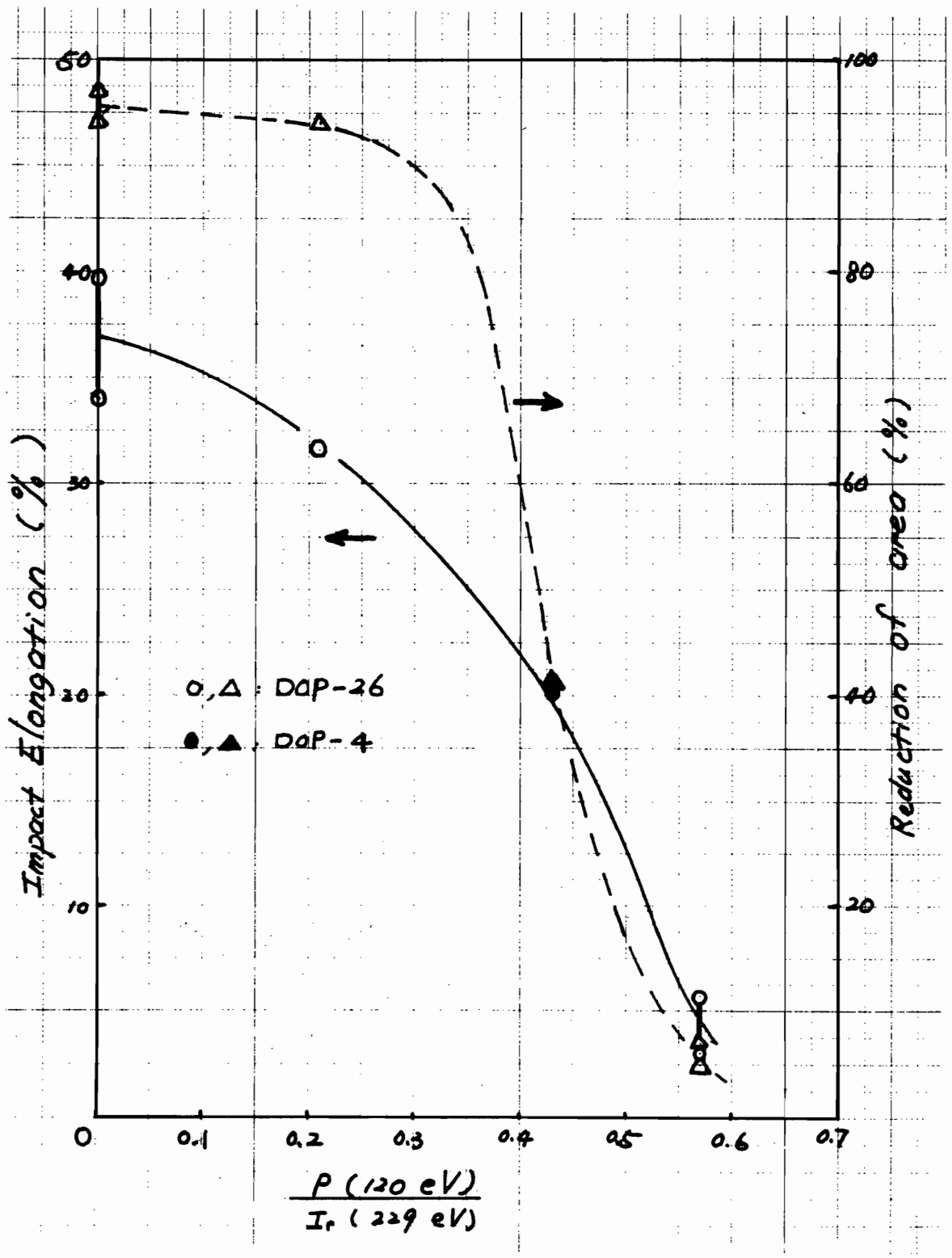

Fig. 3. Plot of impact elongation and reduction of area of DOP-26 and DOP-4 as a function of Auger intensity ratio, P(120 eV)/Ir(229 eV).

AES Analysis of P-Doped DOP-26 (C. L. White and R. A. Padgett)

Two samples of P-doped DOP-26 from the sholder sections of uniaxial impact specimens were analyzed using Auger electron spectroscopy (AES). Sample 800013 was taken from an impact specimen designated OLMF-8A that had been annealed 18 h/1500°C/vac then annealed for 1 h/1500°C in a graphite crucible with P_2O_5.[1] Sample 800014 was taken from a uniaxial impact specimen designated OLMF-8AB that had been given the same annealing and P-doping as 800013, plus a 2 h/1500°C/vac anneal just prior to impact testing.

AES results in samples 800013 and 800014 are summarized in Figs. 4 and 5. Average P(120 eV)/Ir(229 eV) peak height ratios on the fresh fracture surface of sample 800013 (as doped) ranged between 0.5 and 0.65. Alternate AES analysis and inert ion sputtering showed the P-rich region at the grain boundaries to be only a few atom layers thick. The P(120 eV) Auger peak was undetectable after removing approximately 14 atom layers by inert ion sputtering.

Average P(120 eV)/Ir(229 eV) peak height ratios on the fresh fracture surface of sample 800014 (doped + vacuum annealed) ranged between 0.15 and 0.3. These P-levels, while easily detectable, are much lower than for the "as doped" sample. Sputter profiling showed that the P-rich region on this sample was also confined to within a few atom layers of the grain boundaries.

These results, along with uniaxial impact test results, confirm our earlier conclusions that: (1) P segregates strongly to grain boundaries in iridium alloys, (2) P segregation seriously degrades high temperature impact ductility, and (3) P can be removed (at least partially) by vacuum annealing.

Development of Pt-Base Alloys (J. R. Keiser and J. F. Newsome)

The purpose of this work is to develop platinum-base alloys having a high eutectic temperature with graphite as fuel-cladding materials for future flight missions. The first portion of the study consisted of a determination of the eutectic temperature with graphite for several platinum-base alloys. Alloys whose measured graphite eutectic temperature was higher than that of Pt-30 wt % Rh or Pt-3008 include Pt-16 wt % W, Pt-16 wt % Re and Pt-30 wt % Ru. On the basis of these results and previous knowledge of the mechanical properties of several platinum-base alloys, four alloys were selected for study of their fabricability. The four alloys (Pt-8 wt % Re, Pt-16 wt % Re, Pt-15 wt % Ru, and Pt-30 wt % Ru) were checked for fabricability by hot rolling a button of the alloy to 0.76 mm (0.030 in.). All four alloys were successfully rolled without cracking.

---

[1] All P-doping was performed at LASL.

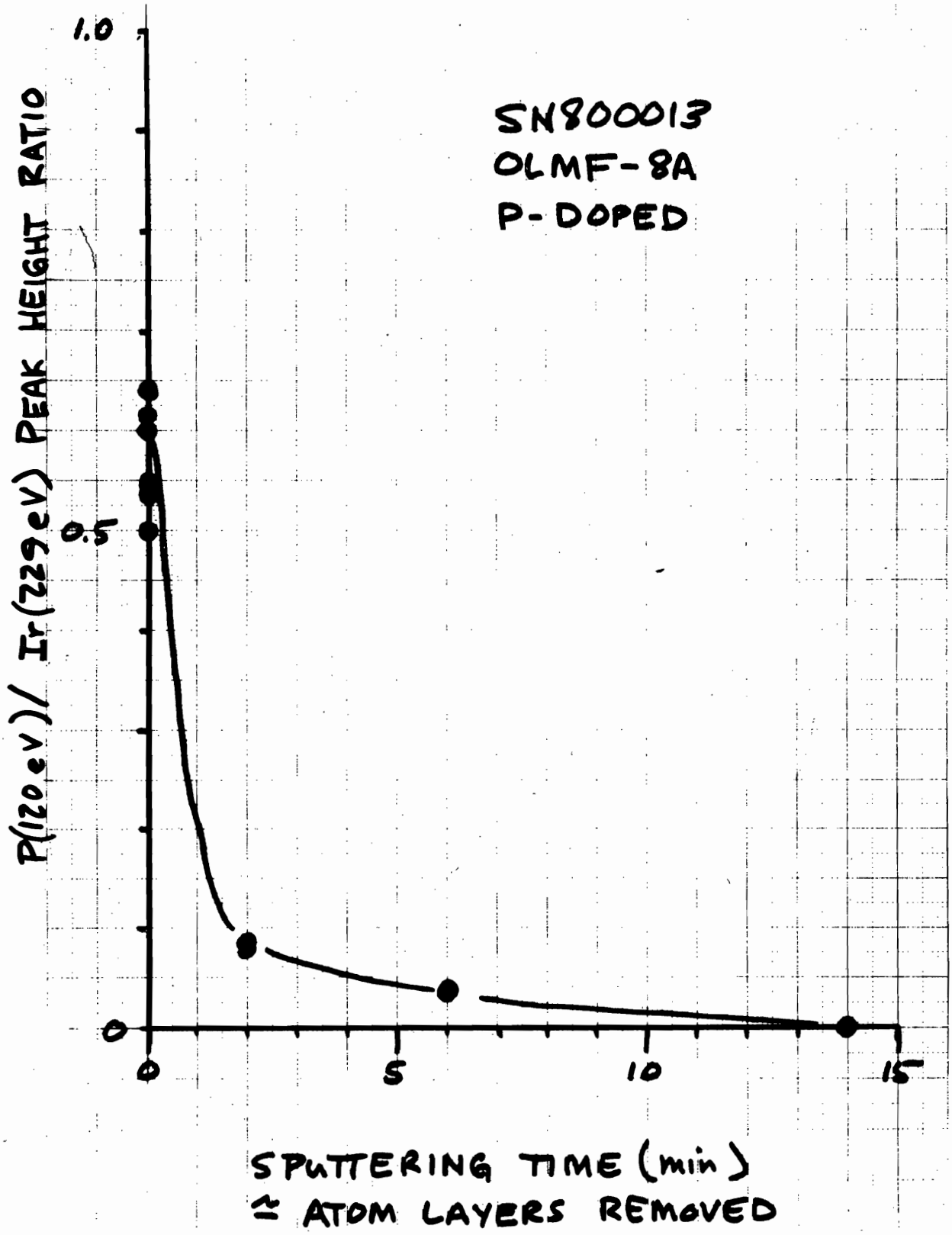

Fig. 4. Plot of P(120 eV)/Ir(229 eV) peak height ratio vs sputtering time for sample 800013.

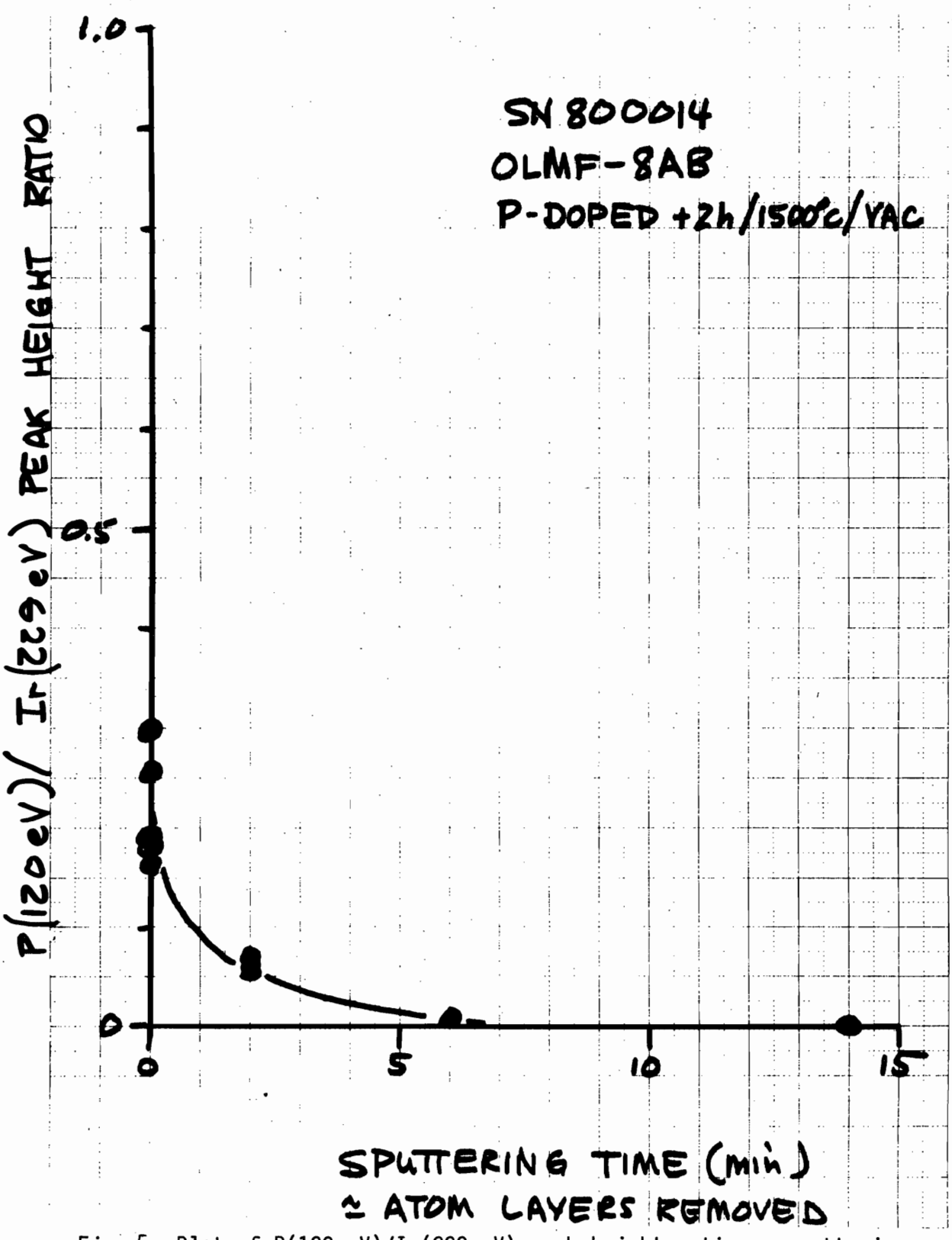

Fig. 5. Plot of P(120 eV)/Ir(229 eV) peak height ratio vs sputtering time for sample 800014.

Tensile specimens have been punched and plans call for them to be impact-tested. Following impact testing, small ingots will be made from the more promising alloys to permit further characterization of the alloys' tensile properties.

Impact Behavior of Mo and Mo-Re Alloys (H. Inouye)

The feasibility of using Mo and Mo-Re alloys as the cladding for the PuO_2 in isotopic heat sources is being explored. Table 5 shows that the impact ductility of arc-cast molybdenum is superior to electron-beam melted Mo-33 Re(w/o) between 400–800°C. The data further show a moderate reduction in the ductility of molybdenum on increasing the test velocity from 10^{-5} to 85 m/sec but virtually no effect caused by the test temperature. On the other hand, the data suggest that both the test temperature and velocity strongly affect the ductility of Mo-33 Re.

Table 5. Effect of Test Velocity and Temperature on the Ductility of Mo and Mo-33 Re Alloys

Alloy	Test Temperature (°C)	Test Velocity	
		(10^{-5} m/sec)	(85 m/sec)
Mo[a]	25	35[c]	----
	400	55[c]	34.9
	600	55[c]	25.6
	800	46.0	38.7
	1350	55[c]	37.2
Mo-33 Re[b]	25	12.8	----
	400	----	5.8
	600	----	13.1
	800	----	17.7
	100	36.4	----

[a]0.51 mm-thick sheet annealed 1 h at 1200°C.

[b]0.63 mm-thick sheet annealed 3 h at 1600°C.

[c]Aged 100 h in vacuum at 1150°C (from ORNL-5431).

Important Meetings

1. D. E. Harasyn, R. L. Heestand, C. T. Liu, A. E. Pasto, A. C. Schaffhauser, and C. L. White attended the 3rd meeting of MHFT Task Force held at ORNL, February 14, 1980.

2. D. E. Harasyn and A. C. Shaffhauser presented the MHFT Task Force summary to ANSP/DOE on February 29, 1980.

ISOTOPE FUEL DEVELOPMENT

(Activity AE 15 35 00 0, WPAS 02314)

R. S. Crouse

$^{90}SrF_2$ Compatibility (R. S. Crouse)

The 30,000 h compatibility capsules from PNL are awaiting disassembly.

TERRESTRIAL RADIOISOTOPE APPLICATIONS DEVELOPMENT

(Activity AE 15 35 00 0, WPAS 01367)

F. N. Case, K. W. Haff, and F. J. Schultz

Cesium-137 Low Solubility Compounds

The instrumentation and equipment required for characterization of the ^{137}Cs pollucite pellets were prepared and transported to a storage area near the hot cell designated for this work. The equipment transported includes four Soxhlet extractors, two water manifolds, water lines, calorimeter, saw and its accompanying off-gas scrubber system, thermopile cord, evacuation flask, constant temperature bath, strip chart recorder, and pellet tweezers.

The calorimeter, pellet tweezers, and the two water manifolds were transferred into the hot cell and the thermopile cord and the water lines were connected to the calorimeter. After the initial cool down of the constant temperature bath it was noticed that the bath was not being controlled by the thermostat. Upon closer examination the thermostat unit was found to be irreparably damaged. The part has been ordered and the scheduled receival date is mid-March.

Leach testing of the three sections of tracer level ^{137}Cs pollucite pellets continued this month. The leach rate of each pellet section is given in Table 6.

Table 6. Tracer Level Cesium-137 Pollucite Pellet Leach Rates

Pellet No.	Accumulated Leaching Period (days)	Leach Rate (g/cm^{-2}-day^{-1})
39	254	29.4×10^{-6}
40	254	5.70×10^{-6}
41	254	18.0×10^{-6}

The above leach rates fall within the previously reported ranges for the steady state values.

Plans to irradiate the three tracer level ^{137}Cs pollucite pellets in an intense gamma field were discussed. After irradiation the pellet sections would be retested under the same conditions as the unirradiated pellets to determine the effects of ionizing radiation on the pellets integrity with regard to leachability.

Examination of WESF Cesium Capsule

The metallurgical examination of the WESF cesium capsule has been completed by the High Radiation Level Examination Laboratory. The results of this examination are being tabulated and the photographs taken are being developed. A complete report on the examination will be presented next month.

Krypton-85 Light Source Development

Four light sources were prepared with 28.5% enriched ^{85}Kr. Each source contained ∿10 Ci of ^{85}Kr. Two were loaded with yellow-green phosphor, one with blue phosphor, and one with red phosphor. One of the yellow-green lights was determined to be leaking and was unloaded to recover the ^{85}Kr. The leakage problem was overcome by making the seal-off section of the quartz spiral smaller prior to filling with ^{85}Kr.

One reflector and lucite light pipe was fabricated for use in testing the light sources. The light pipe functioned well, however, a new design is being fabricated in an attempt to improve the visibility of light emitted at a near horizontal view of the dome of the light pipe. Light visibility when the dome is viewed from above or 15° above horizontal is excellent.

A light tight container was equipped with a photo diode for use in making comparative light output measurements. This will permit a numerical evaluation in units of electrical current for measurement of light output of sources and efficiency of light pipes.

A comparison of the ORNL lights was made with the light prepared by American Atomics and demonstrated at Andrews Air Force Base last spring. The American Atomics light originally contained 17 Ci of 11% enriched ^{85}Kr and is now decayed to 13.9 Ci. For comparison purposes the light output was normalized to curies of ^{85}Kr present in the light source. With curies as a constant, improvements in light output are assumed to be a result of geometry and phosphor differences. The quartz spiral in which the red phosphor was encapsulated was fabricated with a quartz tube obtained from a supplier different than that used for the other spirals. The section of the light source that contained this quartz darkened after filling and the light output is reduced. A new source will be fabricated and a quality control step will be introduced to gamma irradiate quartz tubing prior to filling to determine resistance to gamma ray discoloration.

If we assume an index of 100 for the American Atomics light tested at Andrews Air Force Base last spring, a comparison with the ORNL lights is as follows:

American Atomics	Yellow-green	100
ORNL	Yellow-green	266
ORNL	Blue	288

Since the American Atomics light lost ∿35% of its light output after one year and if we assume a similar light loss from the ORNL sources, the comparative values would be as follows.

American Atomics	Yellow-green	100
ORNL	Yellow-green	172
ORNL	Blue	187

Thus, we have achieved a nearly doubling of light per curie of ^{85}Kr with the ORNL design. There are two areas of further improvement to be anticipated: 1) the use of 48% ^{85}Kr should improve the output by 70% and 2) better control of the phosphor particle size and coating density should provide some 10 to 30% improvement. Thus, we may obtain an overall improvement of about two times greater than the light output per curie of ^{85}Kr when compared with the American Atomics light.

BENEFICIAL APPLICATIONS OF RADIATION TECHNOLOGY

(Activity AE 15 35 00 0, WPAS BART001)

C. S. Sims

On January 15, 1980, ORNL's BART Program was assigned the task of assessing the current technical status of the Cs-137 irradiation technology program. That program has been ongoing for several years at Sandia Laboratories and several other contractors (e.g., BDM, CH_2M Hill, and New Mexico State University) have been associated with it. It includes diverse areas of technology all centrally related to the irradiation and beneficial use of sewage sludge.

An assessment team with ORNL personnel familiar with the several areas of technology associated with the existing program was assembled. They reviewed the pertinent literature, visited the Sandia site on February 12–13 where a program review was conducted and discussions with individual workers were held, wrote assessments and made recommendations within their area of expertise, and submitted their results to C. S. Sims (BART Program Manager) by February 27. Their individual reports constitute the preliminary assessment.

The technical areas receiving the most comments were pathogen reduction, pathways analysis/risk assessment, and concerns about heavy metals in sludges applied to crop lands and used as an animal feed supplement.

INTERNAL DISTRIBUTION

1. E. E. Bloom
2. G. W. Brassell
3. C. R. Brinkman
4. J. A. Carter
5. F. N. Case
6. R. S. Crouse
7. J. E. Cunningham
8. S. A. David
9. J. H. DeVan
10. R. G. Donnelly
11. W. P. Eatherly
12. J. I. Federer
13. G. M. Goodwin
14. K. W. Haff
15. J. P. Hammond
16. D. E. Harasyn
17. W. O. Harms
18. R. L. Heestand
19. M. R. Hill
20. J. R. Keiser
21. J. W. Koger
22. H. Inouye
23. E. Lamb
24. C. T. Liu
25. D. L. McElroy
26. C. D. Montgomery
27. T. K. Roche
28–32. A. C. Schaffhauser
33. C. S. Sims
34. G. M. Slaughter
35. J. O. Stiegler
36. V. J. Tennery
37. D. B. Trauger
38. G. C. Wei
39. J. R. Weir, Jr.
40. C. L. White
41–45. Laboratory Records
46. Laboratory Records, ORNL RC
47. ORNL Patent Office

EXTERNAL DISTRIBUTION

48–59. DOE Division of Advanced Nuclear Systems and Projects, Washington, DC 20545

G. L. Bennett
R. C. Brouns
F. M. Dieringer
N. Goldenberg
J. S. Griffo
W. D. Kenney
J. J. Lombardo
R. B. Morrow
P. A. O'Riordan
W. C. Remini
B. J. Rock
C. O. Tarr

60–61. DOE Albuquerque Operations Office, P.O. Box 5400, Albuquerque, NM 87115

D. K. Nowlin
D. Plymale

62–63. DOE Oak Ridge Operations Office, P.O. Box E, Oak Ridge, TN 37830

J. A. Lenhard
J. Pidkowicz

64–65. DOE San Francisco Operations Office, 1333 Broadway, Wells Fargo Building, Oakland, CA 94612

L. Lanni
W. L. Von Flue

66–67. DOE Savannah River Operations Office, P.O. Box A, Aiken, SC 29801

W. T. Goldston
W. D. Sandberg

68. DOE Dayton Area Office, P.O. Box 66, Miamisburg, OH 45342

H. N. Hill

69. Air Force Weapons Laboratory, Kirtland Air Force Base, DYUS, Albuquerque, NM 87116

Michael Seaton

70–71. Battelle Columbus Laboratories, 505 King Ave., Columbus, OH 43201

E. L. Foster
I. M. Grinberg

72–73. E. I. du Pont de Nemours, Savannah River Plant, Aiken, SC 29801

R. A. Brownback
W. R. Kanne

74–75. E. I. du Pont de Nemours, Savannah River Laboratory, Aiken, SC 29801

R. T. Huntoon
R. H. Tait

76–77. Fairchild Industries, 20301 Century Blvd., Germantown, MD 20767

M. Eck
A. Schock

78. General Atomic Co., P.O. Box 81608, San Diego, CA 92138

N. B. Elsner

79–81. General Electric Co., Valley Forge Space Center, P.O. Box 8048, Philadelphia, PA 19101

V. Haley
R. J. Hemler
C. W. Whitmore

82–84. Jet Propulsion Laboratory, California Institute of Technology, 4800 Oak Grove Drive, Pasadena, CA 91103

R. W. Campbell
J. E. Mondt
A. E. Wolfe

85. Johns Hopkins University, Applied Physics Laboratory, Johns Hopkins Road, Laurel, MD 20810

J. C. Hagan

86–88. Los Alamos Scientific Laboratory, P.O. Box 1663, Los Alamos, NM 87545

R. D. Baker
S. E. Bronisz
S. S. Hecker

89–92. Minnesota Mining and Manufacturing Co., St. Paul, MN 55101

R. B. Ericson
E. F. Hampl
J. D. Hinderman
W. C. Mitchell

93–94. Monsanto Research Corp., P.O. Box 32, Miamisburg, OH 45342

E. W. Johnson
W. C. Wyder

95. Sundstrand Energy Systems, 4747 Harrison Ave., Rockford, IL 61101

E. Krueger

96–97. Teledyne Energy Systems, 110 W. Timonium Rd., Timonium, MD 21093

W. J. Barnett
W. E. Osmeyer